

K-vacancy production in heavy-ion collisions. I. Experimental results for $Z \geq 35$ projectiles*

W. E. Meyerhof, Robert Anholt, T. K. Saylor,[†] S. M. Lazarus,[‡] and A. Little[§]

Department of Physics, Stanford University, Stanford, California 94305

L. F. Chase, Jr.

Lockheed Palo Alto Research Laboratory, Palo Alto, California 94304

(Received 10 June 1976; revised manuscript received 9 August 1976)

We have determined projectile and target K x-ray cross sections from a variety of targets spanning the periodic table and bombarded by 12–60-MeV Br, 200–330-MeV Kr, 15–80-MeV I, 326–470-MeV Xe, and 90–110-MeV Pb. Most targets were thick solids, but, to assure proper extraction of cross sections, some thin solid and gas targets have also been used. The present paper mainly gives experimental details and describes the method of cross-section determination. In subsequent papers various features of the target dependence of the cross section will be examined in terms of atomic and molecular models of inner-shell excitation processes.

I. INTRODUCTION

In the present series of papers we wish to examine the gross features of K -vacancy production mechanisms in heavy-ion collisions. The work was originally undertaken to obtain a quantitative understanding of molecular-orbital (MO) K x-ray spectra,¹ but the present work is restricted to separated-atom (SA) K x-ray formation.

Mechanisms of K -vacancy production have been examined theoretically using as basis atomic or MO wave functions.² The limitations of each of these approaches have been discussed.³ In essence, atomic models are appropriate for target x-ray production if $Z_1 \ll Z_2$, where Z_1 and Z_2 refer to the projectile and target atoms, respectively. Molecular models are most useful if $Z_1 \approx Z_2$ and $v_1 < v_K$, where v_1 and v_K are the projectile speed and the target K -electron Bohr velocity, respectively. Using the method of perturbed stationary states, Basbas *et al.*⁴ have shown how the atomic approach can be extended into the molecular domain, essentially by modifying the former to include binding-energy effects. Polarization effects have also been considered.⁵ A different relation between the two models has recently been obtained by Briggs.⁶

The present paper (I) describes the experimental determination of K -vacancy cross sections and points out common features in the Z_2 dependence of cross sections for a given Z_1 and E_1 (bombarding energy). In future work (paper II) the projectile and target cross sections close to symmetry will be examined in terms of excitations from the $2p\sigma$ MO⁷ and in terms of K -vacancy sharing.^{8,9} In paper III, the cross section of the higher- Z collision partner far from symmetry will be discussed in terms of excitation from the $1s\sigma$ MO. The gradual,

experimental transition between the atomic and molecular domains will be pointed out. In paper IV, the cross section of the lower- Z collision partner far from symmetry will be considered in the light of the K - L level-matching mechanism suggested by Barat and Lichten.⁷

II. EXPERIMENT

Beams of Br and I were produced at the Stanford FN tandem Van de Graaff accelerator, Kr and Xe at the Berkeley Superhilac, and Pb at the Brookhaven MP tandem Van de Graaff accelerator. In most cases, the beam was directed onto a thick target placed at 45° with respect to the beam axis. The target chamber acted as a Faraday cup. An electron suppressor was located between a beam collimator and the target chamber. At Berkeley, the current integration was checked by comparing the experimental yields of Coulomb-excited nuclear γ rays from ¹⁵⁴Sm and ²³⁸U with theoretical estimates.¹⁰ Agreement to within 20% was found.

Si(Li), intrinsic Ge and Ge(Li) detectors were used, depending on the energy and intensity of the x rays to be detected. The detector efficiencies were calibrated with standard radioactive sources. In the energy range from 5 to 14 keV, relative x-ray fluorescence yields from thick x-ray scatterers were used for the calibration.¹¹ Calibrated Al absorbers eliminated unwanted low-energy radiations.

In most cases cross sections were extracted from thick-target yields by the Merzbacher-Lewis formula,¹² as described in Appendix A. Straggling and recoil effects were checked with the convenient formulas of Brandt and Laubert,¹³ and were found to be negligible in all collision systems examined

by us (see Appendix B). To check our method of extracting cross sections, we made several measurements with weighed thin targets, using 47-MeV I, and 326- and 470-MeV Xe beams. Most thin-target cross sections agreed within 10 to 20% with the thick-target cross sections.

A few measurements were made with Kr and Xe, using gas targets confined in a 4.4-cm-long cell covered with a 2.5- μm -thick Ni entrance window. Only a central 2-cm-long section of the cell could be seen by the x-ray detector. The pressure was kept between 5 and 200 Torr, to keep the energy loss in the gas to reasonable values. In certain cases one expects a gas-target cross section to be smaller than a solid-target cross section,¹⁴ as will be discussed in paper II. But in other situations, e.g., for higher- Z cross sections in very asymmetric collisions, no solid-state effects are expected, and here our gas cross sections agree within 20 to 30% with cross sections for solid targets of adjacent elements.

Errors contributing to uncertainties in our cross sections consist of the following components: beam integration $\pm 10\%$, detection efficiency $\pm 15\%$, dead-time effects less than $\pm 5\%$, absorption less than $\pm 15\%$, and conversion from thick-target yield to cross section $\pm 20\%$, giving an overall estimated error of approximately $\pm 30\%$. In the case of low yields ($< 10^{-8}$ photons/projectile), uncertainties caused by room background subtraction and poor statistics could cause errors as large as a factor of 2 or 3. Also, in the region of strongly deformed nuclei ($Z \approx 60$ to 75 and $Z > 90$), internal conversion decay from nuclear Coulomb-excited states can produce x rays of comparable or greater intensity than the SA x rays from the atomic collision processes. In some cases, the detected nuclear γ rays could be used to estimate the contribution of internal conversion x rays to the total x-ray yield. If the internal conversion x-ray yield is large, a large uncertainty is attached to the resultant atomic x-ray yield.

All K x-ray cross sections were converted to K -vacancy yields by using neutral-atom fluorescence yields.¹⁵ For $Z > 20$ this should not introduce additional uncertainties in the cross section exceeding 10%, since K fluorescence yields differ from neutral-atom yields appreciably only if the L shell is practically empty.¹⁶ This situation occurs only rarely in solid targets.¹⁷

III. RESULTS

Figures 1–6 give sample projectile and target K -vacancy cross-section data from our work, as well as other cross sections interpolated or extrapolated to equal relative projectile-target veloci-

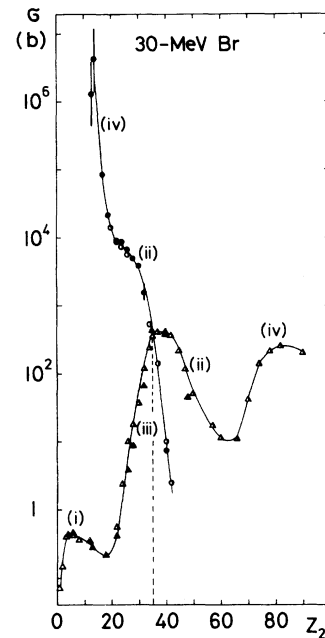


FIG. 1. Projectile and target K -vacancy cross sections for 30-MeV Br. Symbols: \blacktriangle , thick-target projectile cross section, from present experiment; \triangle , projectile cross sections from inverse collisions extrapolated to same projectile velocity (see text for references); \bullet , thick-target target cross sections; \blacktriangle and \circ , projectile and target cross sections, respectively, extrapolated from Ref. 22. Typical errors $\pm 30\%$, except where indicated otherwise. Typical features of the cross sections, marked by roman numerals, are discussed in the text. Curves are only to guide the eye. Dashed vertical line indicates symmetric collision.

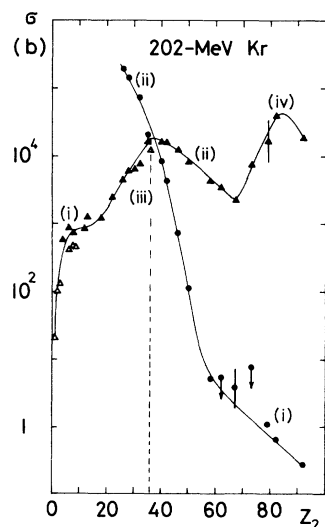


FIG. 2. Projectile and target K -vacancy cross sections for 202-MeV ^{84}Kr . See caption for Fig. 1, except that here symbol \triangle represents projectile cross section extrapolated from 135- and 156-MeV Kr data.

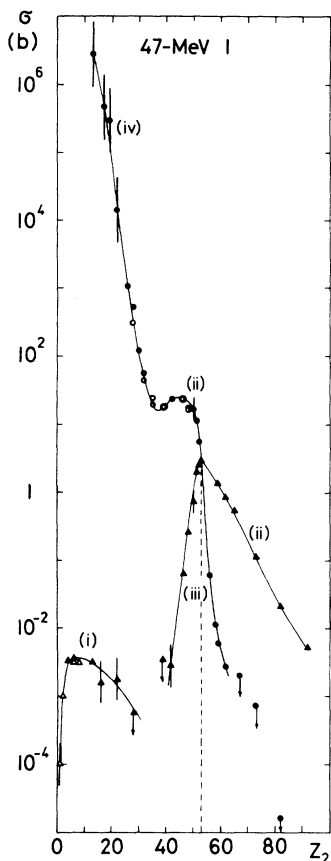


FIG. 3. Projectile and target K -vacancy cross sections for 47-MeV I. See caption for Fig. 1, except that here Δ and \bullet represent thin-target data for projectile and target, respectively.

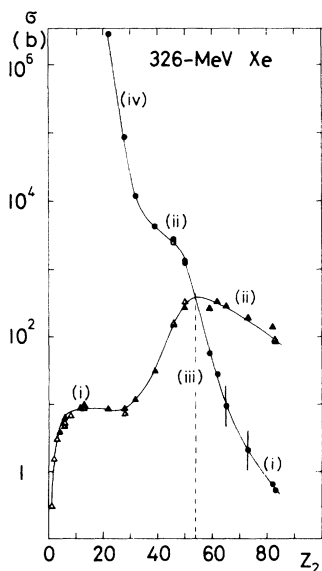


FIG. 4. Projectile and target K -vacancy cross sections for 326-MeV ^{136}Xe . See caption for Fig. 1, except that here, Δ and \bullet represent thin-target data for projectile and target, respectively.

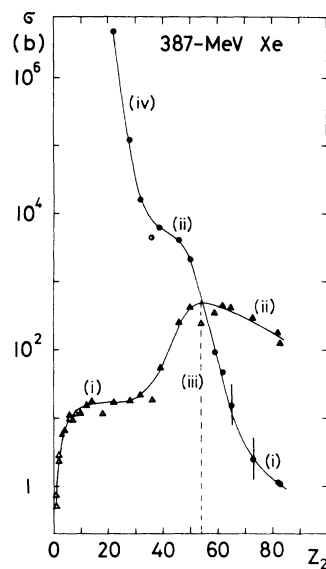


FIG. 5. Projectile and target K -vacancy cross sections for 387-MeV ^{136}Xe . See caption for Fig. 1, except that here solid symbols represent interpolation of 326- and 470-MeV data, and Δ and \bullet represent gas-target data for projectile and target, respectively.

ty.¹⁸⁻²² These extrapolations were always made on $\log\sigma$ -vs- $\log E_1$ plots (σ is the K -vacancy cross section, E_1 the bombarding energy). At low values of Z_2 , the Z_1 cross sections could be obtained from inverse collisions $Z_2 \rightarrow Z_1$.¹⁸⁻²² The match up with our thick-target cross sections is generally satisfactory (see Figs. 1-5, $1 \leq Z_2 \leq 8$, and Fig. 3, $Z_2 = 28, 35$). In this region our gas-target data also

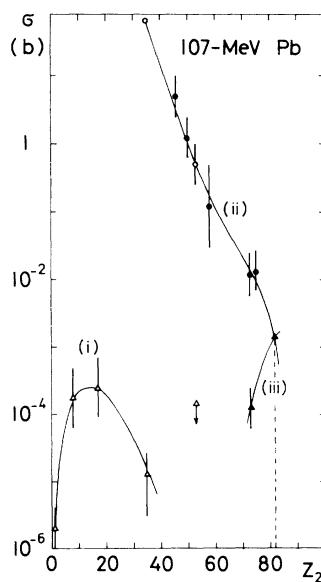


FIG. 6. Projectile and target K -vacancy cross sections for 107-MeV Pb. See caption for Fig. 1.

agrees reasonably well with inverse collision data and with thick-target cross sections (Fig. 5, $1 \leq Z_2 \leq 10$).

In general, the thin-target and thick-target cross sections agree within expected error (see Figs. 3 and 4). On the other hand, near symmetry ($Z_1 \approx Z_2$), the gas-target cross sections appear to be lower, by as much as a factor $\frac{1}{2}$, from the trend of the solid-target data (see Figs. 2 and 5). This may be due to solid-state effects,¹⁴ as discussed in paper II.

The Pb data (Fig. 6) are quite sparse and inaccurate because of low cross sections or uncertain extrapolations. We show this data only to point out that the trends found in other cross sections are present here also.

IV. DISCUSSION

Since the values of v/v_K , where v_K refers to the projectile, are all appreciably less than unity (from 0.06 for 107-MeV Pb to 0.30 for 202-MeV Kr), and since, over most of the region of Z_2 examined, Z_1 and Z_2 have comparable magnitudes, it is appropriate to discuss the cross sections shown in Figs. 1–6 in terms of the molecular model.^{3,7} Figure 7 gives a schematic correlation diagram⁷ for symmetric and asymmetric collisions. Only those levels and excitation processes are indicated which are relevant to the present discussion.

The common features in the cross sections which we wish to discuss qualitatively in terms of basic MO excitation processes are marked with roman

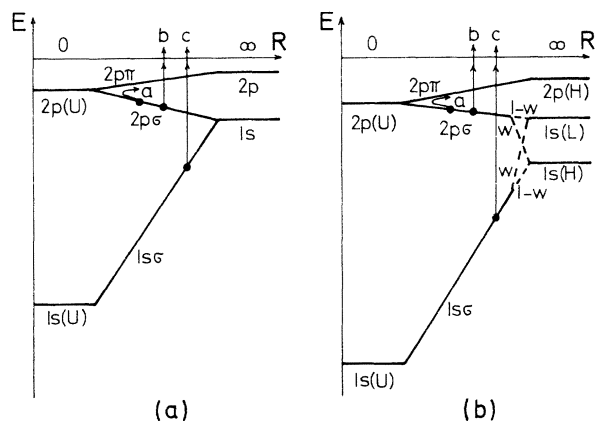


FIG. 7. Schematic correlation diagrams for symmetric (a) and asymmetric (b) collisions. Only levels relevant to the present discussion are shown. Three excitation processes a, b, and c are indicated, which are discussed in the text. For asymmetric collisions the vacancy transfer probability w plays an important role. The letters H, L, and U refer to the higher- Z , lower- Z collision partners and the united atom, respectively.

numerals (i) to (iv) on Figs. 1 to 6. In subsequent papers, quantitative comparisons with various theories are presented.

Region (i). For very low values of Z_2 , Z_1 is the higher- Z partner and its cross section is appropriately compared with “atomic” theories. It has been shown that perturbed stationary-state theory with atomic wave functions, which includes binding energy and polarization effects,^{4–6} can explain the Z_1 cross sections ($Z_1 > Z_2$!) in region (i) up to values of Z_2 between 10 and 20.^{19–21} As Z_2 increases beyond this region, the theoretical cross sections fall increasingly below experiment, probably because of an overestimate of the binding-energy effect.²³

From the molecular point of view, the cross sections in region (i) represent the excitation from the $1s\sigma$ MO to the continuum, and possibly to high-lying vacant states (process c on Fig. 7).²⁴ Hansen²⁵ and Foster *et al.*²⁶ have proposed modifications of the binary encounter theory to simulate the molecular effects. These modifications, for which Briggs⁶ has attempted to find a theoretical basis, as well as other semiempirical approaches proposed by us,²³ will be discussed in paper III.

There is a second region where excitation from the $1s\sigma$ MO is expected to play a dominant role. This occurs for the target cross section for very large values of Z_2 (e.g., Fig. 2, $Z_2 \approx 60$; Figs. 4 and 5 $Z_2 \approx 70$). Here, relativistic effects are extremely important. In paper III an estimate will be presented which makes it possible to find a quantitative explanation for these cross sections.

We note the good agreement of the $Z_1 \rightarrow Z_2$ cross sections in region (i) with the $Z_2 \rightarrow Z_1$ cross sections (Figs. 1–4), indicating the absence of solid-state effects.¹⁴ The one exception is the case of 202-MeV Kr, where the $Z_1 \rightarrow Z_2$ cross sections exceed the $Z_2 \rightarrow Z_1$ cross sections by as much as a factor 2 (Fig. 2, $Z_2 < 10$). Since the $Z_2 \rightarrow Z_1$ cross sections were extrapolated from solid-target data,^{19–21} one might suspect that capture of (higher- Z) target K electrons into (lower- Z) projectile K vacancies could enhance the $Z_2 \rightarrow Z_1$ cross section over the $Z_1 \rightarrow Z_2$ cross section.²⁷ Experimentally the opposite situation is found. Hence it is more likely that stripping or excitation of the Kr projectile in the $Z_1 \rightarrow Z_2$ collisions produces a reduction of the effective K excitation energy and consequently, an increase in the K -vacancy production cross section.²⁸ Furthermore, stripping or excitation of Kr L electrons could increase the fluorescence yield in $Z_1 \rightarrow Z_2$ collisions, compared to $Z_2 \rightarrow Z_1$ collisions.

We also want to draw attention to the fact that in region (i) the 47-MeV I data are affected materially by Coulomb excitation of the 58-keV state of ¹²⁷I.

Contributions to the x-ray yield from internal-conversion decay of this state have been subtracted in Fig. 3. They account for the entire experimental yield between $Z_2=28$ and 40. They had not been subtracted in Fig. 2 of Ref. 8, nor in Fig. 3 of Ref. 24, which are therefore in error in this region of Z_2 .

Regions (ii) and (iii). It has been pointed out by Purser²⁹ that in a fairly wide region of Z_2 spanning symmetry, the *sum* of the projectile and target cross sections lie on a smooth curve as a function of Z_2 , contrary to the individual cross sections. In paper II, examples of such plots will be given. If the cross section of the higher- Z collision partner drops to small values, i.e., outside of region (iii), this smooth curve represents the cross-section trend of the lower- Z collision partner [regions (ii) in Figs. 1–6].

These features can be understood in terms of the molecular processes sketched in Fig. 7. The $2p\sigma$ MO can receive vacancies by the Fano-Lichten electron promotion mechanism (a),⁷ if vacancies are somehow produced in the $2p\pi$ MO,³⁰ and by the direct excitation process (b).^{6,24,26} These processes, which will be detailed in paper II, both are expected to be smooth functions of Z_2 across the region of symmetry.

On the outgoing part of the collision, the $2p\sigma$ vacancies are shared between the higher- Z and lower- Z 1s states with relative probabilities w and $1-w$, respectively, where $w \leq \frac{1}{2}$.^{8,9} Hence the summed K -vacancy cross section for both collision partners represents the total $2p\sigma$ vacancy cross section on the outgoing part of the collision, plus a very small contribution from process (c). Empirical³¹ and semiempirical²⁶ scaling laws for the Z_2 and E_1 dependence of the $2p\sigma$ cross sections have been proposed, some quite successful, as shown in paper II. In Fig. 3, the variation of the target cross section between $Z_2=35$ and 50 is an exception to the smooth behavior discussed above. Most likely, this is a solid-state effect, as will be discussed in detail in paper II.

Close to symmetry, in region (iii), the vacancy sharing process can account for the Z_2 dependence of the higher- Z K -vacancy cross section,⁸ except in the case of 202-MeV Kr, when the simple vacancy sharing formula appears to break down perhaps because of the high value of v_1/v_K (see paper II). We attribute the empirical deviations found in Ref 32 to target recoil effects, as discussed in paper II. In very light systems ($Z < 10$), many-electron^{30,33} or electron relaxation effects³⁴ can also affect the vacancy sharing ratio.

Region (iv). In the neighborhood of atomic numbers where the 1s binding energy of the lower- Z collision partner matches the $2p$ binding energies

of the higher- Z partner, dramatic increases in the K -vacancy cross section of the lower- Z partner have been noticed.³⁵ If a given projectile Z_1 bombards a range of targets Z_2 , there are two such level matching regions: (1) where the 1s level of Z_2 matches the $2p$ levels of Z_1 (see Fig. 3; the I $2p$ levels match the K level of $Z_2 \approx 22$), and (2) where the 1s level of Z_1 matches the $2p$ levels of Z_2 (see Figs. 1 and 2; the Br and Kr K levels match the $2p$ levels of $Z_2 \approx 80$).

Barat and Lichten⁷ have discussed the level-matching effect in terms of the molecular model (Fig. 7). Whereas normally the UA $3d$ level correlates with the $2p(H)$ level (neglecting spin-orbit coupling) via the $3d\sigma$ MO (not shown on Fig. 7), if the $1s(L)$ level lies *above* the $2p(H)$ level the $3d\sigma$ MO correlates to the $1s(L)$ level. In the latter case, the $1s(L)$ level can receive the, presumably copious, $3d\sigma$ vacancies, and a large increase in the $1s(L)$ vacancy cross section can occur. Foster *et al.*²⁶ have suggested that the Z_2 dependence of the $1s(L)$ cross section in Br collisions (see Fig. 1) can be understood in terms of a $3d\sigma \rightarrow 2p(H)$, $1s(L)$ vacancy sharing mechanism analogous to the $2p\sigma \rightarrow 1s(L)$, $1s(H)$ vacancy sharing.⁸ An explanation³⁶ of the K - L level-matching processes in terms of a new correlation scheme proposed by Eichler *et al.*³⁷ will be discussed in paper IV.

Summary. In the light of the preceding discussion, we write the K -vacancy cross sections for the higher- and lower- Z collision partners as follows:

$$\sigma(H) = \sigma(1s\sigma) + w\sigma(2p\sigma), \quad (1)$$

$$\sigma(L) = (1-w)\sigma(2p\sigma) + \sigma_{K-L}, \quad (2)$$

where $\sigma(1s\sigma)$ is the $1s\sigma$ excitation cross section of region (i), $\sigma(2p\sigma)$ is the total $2p\sigma$ vacancy cross section on the outgoing part of the collision [regions (ii) and (iii)], w is the K -vacancy sharing ratio^{8,9} and σ_{K-L} is the contribution from K - L level matching [region (iv)]. Equation (1) assumes that the $1s\sigma$ cross section does not participate in the vacancy sharing process,⁸ contrary to what is shown in Fig. 7b, because experimentally one cannot determine $\sigma(1s\sigma)$ except in the region where w is practically zero. In paper IV, a justification will be given for excluding σ_{K-L} from the vacancy sharing process. Papers II, III, and IV will discuss in detail the cross sections $\sigma(2p\sigma)$, $\sigma(1s\sigma)$, and σ_{K-L} , respectively.

V. CONCLUSION

The present work illustrates common features in heavy-ion K -vacancy production. The common features are summarized in Eqs. (1) and (2). Near

symmetry, the cross sections are dominated by the sharing of the $2p\sigma$ vacancies. Far from symmetry, the lower- Z partner profits from K - L level matching, and the higher- Z partner obtains vacancies solely by $1s\sigma$ excitation. The latter process provides an experimental means to study the gradual transition from the atomic to the molecular regime, which is of much theoretical interest.²⁻⁶ In this connection it is important to extend the Pb K -vacancy cross sections measurements (Fig. 6), since they provide the largest region (i). A good understanding of relativistic effects will then be important.³⁸

In lighter systems than those examined by us, one expects the same common features in the K -vacancy cross sections as those found here (e.g., see Ref. 39). The only difference is that the electron promotion process (a) (see Fig. 7) is expected to play an increasingly important role as Z_1 and Z_2 decrease, until for $Z_1, Z_2 < 10$ it completely dominates the $2p\sigma$ vacancy production.³⁰

ACKNOWLEDGMENTS

We are indebted to Dr. Peter Bond, Dr. Richard Diamond, Dr. John Rasmussen, Dr. Frank Stephens and Dr. Baylor Triplett for assistance during various phases of this work. We thank Donald Ramsay for skillful preparation of various thin targets. One of us (W. E. M.) profited from the hospitality of the Nuclear Chemistry Department of the Lawrence Berkeley Laboratory during a sabbatical leave. One of us (R. A.) is indebted to Professor J. Rasmussen for his encouragement and to the Lawrence Berkeley Laboratory for support over many years during the latter part of which some of the present work was done. We appreciate the help of G. Rattazzi and J. S. Dunham during some of the data taking.

APPENDIX A: CROSS-SECTION DETERMINATION

The extraction of x-ray cross sections (σ) from thick-target yields (Y) has been discussed by Taubjerg *et al.*⁴⁰ and conveniently parametrized by Laubert.¹³ We show in Appendix B that recoil and straggling effects are negligible in all collision systems examined by us. In that case, the Merzbacher-Lewis formula¹² is applicable.⁴⁰ For a thick target placed at 45° to the beam direction, viewed by a x-ray detector at 90° ,

$$\sigma(E_1) = \frac{1}{n_2} \left(\frac{dY(E_1)}{dE_1'} \frac{dE_1'}{dx} \right)_{E_1'=E_1} + \frac{\mu Y(E_1)}{n_2}. \quad (\text{A1})$$

Here, n_2 is the number of target atoms per unit volume, E_1 is the incident projectile energy, dE_1'/dx is the differential energy loss of the projectile in the target, and μ is the x-ray absorption

coefficient in the target. In most of our systems the second term in Eq. (A1) contributes no more than a few percent and has been neglected, except in the case of target cross sections for $Z_2 \leq 20$.

It has been pointed out by Schnopper *et al.*⁴¹ that frequently K -vacancy cross sections obey the relation $\sigma \propto E_1^\alpha$, where α is constant over limited regions of E_1 or only weakly dependent on E_1 . Our results show that, for the heavy projectiles and the bombarding energy range used, a similar relationship holds for the thick-target yield Y

$$Y \propto E_1^\beta, \quad (\text{A2})$$

where $\beta = \beta(Z_1, Z_2, E_1)$ is only weakly dependent on E_1 . Figure 8 gives sample plots from our work, illustrating the relationship (A2). With this relationship, Eq. (A1) can be written, for a monoisotopic target and omitting the second term,

$$\sigma(E_1) = \frac{Y(E_1)\beta A_2}{N_0 E_1} \left(\frac{dE_1'}{d(\rho_2 x)} \right)_{E_1'=E_1}, \quad (\text{A3})$$

where A_2 and ρ_2 are the target atomic weight and density, respectively, and N_0 is Avogadro's number.

Since for most collision pairs Z_1, Z_2 we made measurements only at two values of E_1 , we ob-

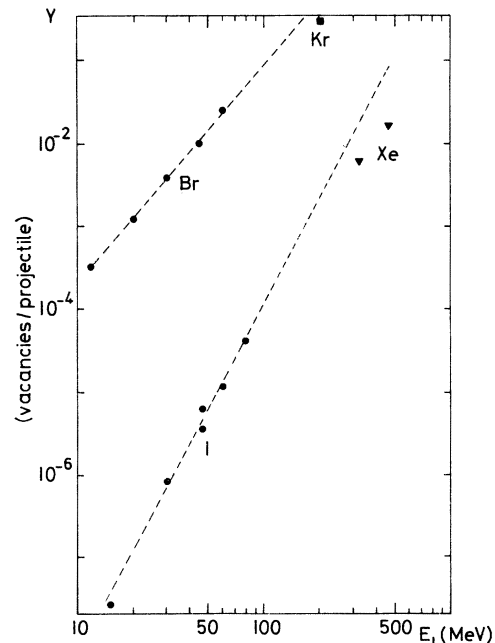


FIG. 8. Typical bombarding energy dependence of thick-target projectile yields for symmetric collisions. The dashed lines represent a power-law dependence of the form (A2) with constant exponent β . These lines are only meant to guide the eye and were *not* used in the β determination, in which the E_1 dependence of β was taken into account.

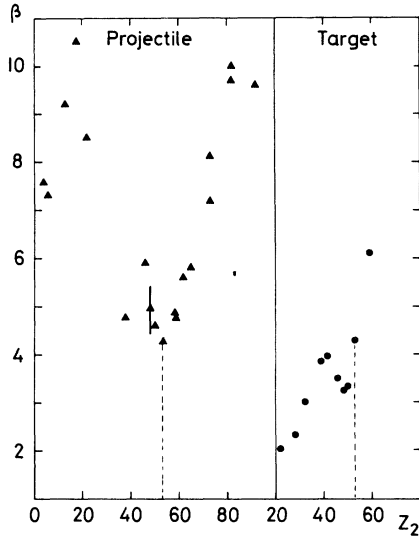


FIG. 9. Values of power-law exponent β [Eq. (A2)] as a function of Z_2 for thick-target projectile and target yields from I collisions between 47 and 62 MeV. Vertical dashed lines indicate symmetric collision. Typical error on β is ± 0.5 .

tained values for β for projectile and target yields in the following manner, accurate to at least 20%. For example, treating Br and Kr as a single projectile species, we assumed that the power law (A2) holds between $E_1 = 30$ and 202 MeV (see Fig. 8). The resulting values of β show relatively regular variations as a function of Z_2 (see Fig. 9),

which can be interpolated if needed. It might be objected that in the cases in which Br and Kr are the higher- Z collision partners, the Z dependence of their cross sections is extremely strong, such as Z^{-12} predicted by the PWBA.¹² But we note that $(36/35)^{12} = 1.4$, and over the E_1 range considered here (30–202 MeV) the yield typically varies by a factor 10^4 . Since

$$\beta = \frac{\log[Y(E'_1)/Y(E''_1)]}{\log(E'_1/E''_1)},$$

the uncertainty of a factor 1.4 in the yield ratio does not affect β by more than a few percent. This is much smaller than systematic errors in β which are as large as 20% (Fig. 9).

For I, measurements were made at 47 and 62 MeV, and for Xe at 326 and 470 MeV, so that β could be determined directly in each case. In the case of Pb, measurements were very tedious, taking as long as 8 hours, and each using up to 20 stripper foils in the Tandem Van de Graaff terminal.³¹ Hence, only the Pb + Pb yields were measured at two energies (88 and 107 MeV). The resulting value of β (≈ 8) was used to determine all other directly measured cross sections on Fig. 6. Judging from the plots in Fig. 9, this introduces uncertainties in the cross sections by a factor of about 2. Within this uncertainty, Fig. 6 indicates that the directly measured cross sections agree with the extrapolated cross sections obtained from inverse collisions.^{18,22}

All energy loss values needed in Eq. (A3) were

TABLE I. Straggling and recoil corrections to K -vacancy cross sections.^a

E_1 (MeV)	Z_1, Z_2	Projectile			Target		R
		σ	K	σ	K		
30	Br + Mg	3.3 (-1)	5.3 (-4)	
30	Br + Fe	3.4 (0)	9.5 (-3)	5.1 (3)	6.4 (0)	2.6 (0)	
30	Br + Zr	3.4 (2)	5.0 (-1)	6.4 (0)	2.1 (-2)	3.3 (-2)	
202	Kr + Be	6.0 (2)	3.3 (-2)	
202	Kr + Fe	4.9 (3)	1.3 (0)	1.9 (5)	2.3 (1)	1.2 (1)	
202	Kr + Zr	1.6 (4)	2.3 (0)	8.3 (3)	2.4 (0)	2.4 (-1)	
202	Kr + Pb	4.0 (4)	1.6 (1)	6.6 (1)	2.9 (-4)	1.1 (-8)	
47	I + Al	3.2 (-3)	1.6 (-5)	2.8 (6)	2.1 (3)	4.5 (3)	
47	I + Ni	<6 (-4)	<4 (-6)	4.0 (2)	6.5 (-1)	5.5 (0)	
47	I + Y	3.6 (-3)	1.8 (-5)	1.8 (1)	6.7 (-2)	2.2 (-1)	
47	I + Pr	1.1 (0)	6.1 (-3)	5.9 (-3)	4.6 (-5)	4.3 (-4)	
47	I + Pb	2.1 (-2)	3.9 (-4)	<1.3 (-5)	<3 (-7)	3 (-9)	
470	Xe + Al	3.2 (1)	4.2 (-3)	
470	Xe + Ni	4.0 (1)	1.2 (-2)	1.8 (5)	2.6 (1)	2.6 (1)	
470	Xe + Y	1.1 (2)	3.0 (-2)	9.3 (3)	1.6 (0)	1.2 (0)	
470	Xe + Pr	5.2 (2)	8.8 (-2)	1.6 (2)	4.1 (-2)	1.6 (-2)	
470	Xe + Pb	2.5 (2)	5.5 (-2)	2.6 (1)	7.9 (-4)	4.0 (-6)	

^a All cross sections in barns. The power of 10 by which each number has to be multiplied is given in parentheses. Typical absolute errors, $\pm 30\%$; relative errors for one projectile, $\pm 20\%$.

taken from Ref. 42, and the corrections suggested in Ref. 43 were applied.

APPENDIX B: STRAGGLING AND RECOIL EFFECTS

As discussed in Refs. 40 and 13, one must subtract from Eq. (A1) a straggling contribution K if the projectile cross section is desired, and straggling and recoil contributions $K+R$ if the target cross section is desired. We specify the formulas of Ref. 13 to the case of pure Rutherford scattering and to a linear velocity dependence of the stopping powers of projectile and (recoiling) target ions in the target material. Substitution of the power law assumption, (A2) then results in the following estimates for K and R :

$$K = 0.131 \left(\frac{Z_1 Z_2 A_1}{A_1 + A_2} \right)^2 \frac{\beta(\beta - 1) Y(E_1)}{E_1^2}, \quad (\text{B1})$$

$$R = 7.59 \times 10^{-7} Z_1^2 Z_2^{5/6} (A_1 + A_2) A_1^{1/2} A_2^{-1} \frac{\sigma(Z_2, Z_2, T_M)}{(l^2 - \frac{1}{4}) E_1^{3/2}}, \quad (\text{B2})$$

where $T_M = 4A_1 A_2 E_1 / (A_1 + A_2)^2$ and the subscripts 1 and 2 refer to projectile and target, respectively. Also, E_1 is in MeV; A is in amu; K , R , and σ are

in barns. In Eq. (B2) the cross section $\sigma(Z_2, Z_2, E)$ is the K -vacancy production cross section for target atoms moving through the target material with the energy E . The derivation of Eq. (B2) assumes that this cross section has a power-law dependence of the form E^l . The symmetric cross-section measurements of Ref. 31 show that the energy dependence is more complicated. It can be parametrized as follows (in barns):

$$\sigma(Z_2, Z_2, E) = \frac{1.76 \times 10^9 Z_2^{-2} \eta^{6.15}}{\eta^4 + 10^{-5} \eta^2 + 1.8 \times 10^{-10}}, \quad (\text{B3})$$

where $\eta = mE/M_2G$, with m the electron mass, M_2 the projectile mass, and G the $2p\sigma$ binding energy at the distance of closest approach in target-target collisions, which is equal to the UA $2p$ binding energy⁴⁴ for sufficiently energetic collisions (see Fig. 7a). Equation (B3) was used in Eq. (B2), and an equivalent l value was computed from $l = d(\log \sigma)/d(\log E)$.

Table I gives sample values for K and R , and compares them with the uncorrected cross section (A3), converted to vacancy cross section. It is clear, even though K and R are not computed accurately, that they are negligible compared to the estimated 30% error on σ .

*Work supported in part by the National Science Foundation, E.R.D.A., and the Lockheed Independent Research Program. A preliminary account of this work was presented at the Second International Conference on Inner-Shell Ionization Phenomena, Freiburg, Germany, 1976.

† Present address: Department of Physics, Rutgers University, New Brunswick, N.J.

‡ Present address: Aeronutronic Ford Corp., Palo Alto, Calif.

§ Present address: Physics Department, State University of New York, Stony Brook, N. Y.

¹W. E. Meyerhof, T. K. Saylor, S. M. Lazarus, A. Little, B. B. Triplett, L. F. Chase, Jr., and R. Anholt, *Phys. Rev. Lett.* **32**, 1279 (1974).

²References can be found in the following review articles: W. Brandt, in *Atomic Physics 3*, edited by S. J. Smith and G. K. Walters (Plenum, New York, 1972), p. 155; J. D. Garcia, R. J. Fortner, and T. M. Kavanagh, *Rev. Mod. Phys.* **45**, 111 (1973); Q. C. Kessel and B. Fastrup, in *Case Studies in Atomic Physics 3*, edited by M. R. C. McDowell and E. W. McDaniel (North Holland, Amsterdam, 1973), p. 137; J. M. Hansteen, in *Advances in Atomic and Molecular Physics*, edited by D. R. Bates and B. Bederson (Academic, New York, 1975), Vol. II, p. 299; J. S. Briggs, *Rep. Prog. Phys.* **39**, 217 (1976).

³D. H. Madison and E. Merzbacher, in *Atomic Inner-Shell Processes*, edited by B. Craseman (Academic, New York, 1975), Vol. I, p. 1.

⁴G. Basbas, W. Brandt, and R. H. Ritchie, *Phys. Rev.*

A **7**, 1971 (1973); G. Basbas, W. Brandt, and R. Laubert, *Phys. Rev. A* **7**, 983 (1973).

⁵W. Brandt, in *Proceedings of the International Conference on Inner-Shell Ionization Phenomena and Future Applications*, edited by R. W. Fink, S. T. Manson, J. M. Palms, and P. Venugopala Rao (U.S.E.R.D.A., Oak Ridge, 1973), Vol. 2, p. 948; and G. Basbas (private communication).

⁶J. S. Briggs, *J. Phys. B* **8**, L485 (1975).

⁷U. Fano and W. Lichten, *Phys. Rev. Lett.* **14**, 627 (1965); W. Lichten, *Phys. Rev.* **164**, 131 (1967); M. Barat and W. Lichten, *Phys. Rev. A* **6**, 211 (1972).

⁸W. E. Meyerhof, *Phys. Rev. Lett.* **31**, 1341 (1973).

⁹K. Taulbjerg and J. S. Briggs, *J. Phys. B* **8**, 1895 (1975); J. S. Briggs and K. Taulbjerg, *J. Phys. B* **8**, 1909 (1975); K. Taulbjerg, J. Vaaben, and B. Fastrup, *Phys. Rev. A* **12**, 2325 (1975). The third reference points out that a discrepancy between the second reference and Ref. 8 has been removed by a recalculation.

¹⁰J. de Boer (private communication). See also A. Winther and J. de Boer, in *Coulomb Excitation*, edited by K. Alder and A. Winther (Academic, New York, 1966), p. 303.

¹¹J. Jaklevic (private communication). X-ray fluorescence yields were taken from W. H. McMaster, N. Kerr-Del Grande, J. H. Mallet, and J. H. Hubbel, University of California Radiation Laboratory, Report No. UCRL 50174, Sec. II, Rev. 1, 1969 (unpublished).

¹²E. Merzbacher and H. W. Lewis, in *Handbuch der Physik*, edited by S. Flügge (Springer Verlag, Berlin, 1958), Vol. 34, p. 166.

- ¹³R. Laubert (private communication); W. Brandt and R. Laubert, *Phys. Rev. A* **11**, 1233 (1975).
- ¹⁴F. W. Saris and D. J. Bierman, *Phys. Lett.* **35A**, 199 (1971); R. C. Der, R. J. Fortner, T. M. Kavanagh, and J. D. Garcia, *Phys. Rev. Lett.* **27**, 1631 (1971); H. O. Lutz, J. Stein, S. Datz, and C. D. Moak, *Phys. Rev. Lett.* **28**, 8 (1972).
- ¹⁵W. Bambynek, B. Crasemann, R. W. Fink, H. U. Freund, H. Mark, C. D. Swift, R. E. Price, and V. P. Rao, *Rev. Mod. Phys.* **44**, 716 (1972).
- ¹⁶C. P. Bhalla, *Phys. Rev. A* **8**, 2877 (1973); F. Hopkins, D. O. Elliott, C. P. Bhalla, and P. Richard, *Phys. Rev. A* **8**, 2952 (1973); C. P. Bhalla, *Phys. Rev. A* **12**, 122 (1975).
- ¹⁷A. R. Knudson, P. Burkhalter, and D. J. Nagel, *Phys. Rev. A* **10**, 2118 (1974).
- ¹⁸C. H. Rutledge and R. L. Watson, *At. Nucl. Data Tables* **12**, 195 (1973); T. J. Gray, *At. Nucl. Data Tables* (to be published).
- ¹⁹F. D. McDaniel and J. L. Duggan, in *Beam Foil Spectroscopy*, edited by I. A. Sellin and D. J. Pegg (Plenum, New York, 1976), Vol. 2, p. 519.
- ²⁰F. D. McDaniel, T. J. Gray, R. V. Gardner, G. M. Light, J. L. Duggan, H. A. Van Rinsvelt, R. D. Lear, G. H. Pepper, J. W. Nelson, and A. R. Zander, *Phys. Rev. A* **12**, 1271 (1975); R. M. Wheeler, R. P. Chaturvedi, J. L. Duggan, J. Tricomi, and P. D. Miller, *Phys. Rev. A* **13**, 958 (1976).
- ²¹T. J. Gray, P. Richard, R. L. Kaufman, T. C. Holloway, R. K. Gardner, G. M. Light, and J. Guertin, *Phys. Rev. A* **13**, 1344 (1976); J. Tricomi, J. L. Duggan, F. D. McDaniel, P. D. Miller, R. P. Chaturvedi, R. M. Wheeler, J. Lin, K. A. Kuenhold, L. A. Rayburn, and S. J. Cippola, *Phys. Rev. A* (to be published).
- ²²H. Kubo, F. C. Jundt, and K. H. Purser, *Phys. Rev. Lett.* **31**, 674 (1973); F. C. Jundt (private communication). The Ni cross sections appear to be consistently too low and have been multiplied by a factor 3, if used here. (This is probably a solid-state effect, as shown in paper II). See R. Laubert, H. Haselton, J. R. Mowat, R. S. Peterson, and I. A. Sellin, *Phys. Rev. A* **11**, 135 (1975).
- ²³W. E. Meyerhof and R. Anholt, in *Abstracts Second International Conference on Inner-Shell Ionization Phenomena, Freiburg, Germany* (University of Freiburg, Germany, 1976), p. 56.
- ²⁴W. E. Meyerhof, *Phys. Rev. A* **10**, 1005 (1974).
- ²⁵J. S. Hansen, *Phys. Rev. A* **8**, 822 (1973).
- ²⁶C. Foster, T. P. Hoogkamer, P. Woerlee, and F. W. Saris, *J. Phys. B* **9**, 1943 (1976).
- ²⁷A. M. Halpern and J. Law, *Phys. Rev. Lett.* **31**, 4 (1973); **31**, 620 (1973); *Phys. Rev. A* **12**, 1776 (1975); J. H. McGuire, *Phys. Rev. A* **8**, 2760 (1973); M. D. Brown, L. D. Ellsworth, J. A. Guffy, T. Chiao, E. W. Pettus, L. M. Winters, and J. R. Macdonald, *Phys. Rev. A* **10**, 1225 (1974); H. D. Betz, in Ref. 23, p. 100; H. Panke, F. Bell, and H. D. Betz, in Ref. 23, p. 101.
- ²⁸E. Laegsgaard (private communication).
- ²⁹K. H. Purser (private communication).
- ³⁰For details of processes which can produce $2p\pi$ vacancies see B. Fastrup, in *The Physics of Electronic and Atomic Collisions*, edited by J. S. Risley and R. Geballe (Univ. of Washington Press, Seattle, 1975), p. 361.
- ³¹W. E. Meyerhof, R. Anholt, T. K. Saylor, and P. D. Bond, *Phys. Rev. A* **11**, 1083 (1975).
- ³²K. W. Jones, F. C. Jundt, G. Guillaume, and P. Fintz, *Phys. Rev. A* **12**, 1232 (1975).
- ³³N. Stolterfoht and U. Leithäuser, *Phys. Rev. Lett.* **36**, 186 (1976); V. Sidis, N. Stolterfoht, and M. Barat, in Ref. 23, p. 68.
- ³⁴B. Fastrup (private communication).
- ³⁵P. Armbruster, E. Röckl, H. J. Specht, and A. Vollmer, *Z. Naturforsch* **19a**, 1301 (1964); H. J. Specht, *Z. Phys.* **185**, 301 (1965).
- ³⁶W. E. Meyerhof, in Ref. 23, p. 62; *Abstracts Fifth International Conference on Atomic Physics, Berkeley, 1976*, edited by R. Marrus, M. H. Prior, and H. A. Shugart (Univ. of California, Berkeley, 1976), p. 64.
- ³⁷J. Eichler, U. Wille, B. Fastrup, and K. Taubjerg, *Phys. Rev. A* **14**, 707 (1976).
- ³⁸P. A. Amundsen, *J. Phys. B* **9**, 971 (1976); P. A. Amundsen, L. Kocbach, and J. M. Hansteen, *J. Phys. B* **9**, L203 (1976).
- ³⁹L. Winters, J. R. Macdonald, M. D. Brown, T. Chiao, L. D. Ellsworth, and E. W. Pettus, *Phys. Rev. Lett.* **31**, 1344 (1973); L. Winters, M. D. Brown, L. D. Ellsworth, E. W. Pettus, and J. R. Macdonald, *Phys. Rev. A* **11**, 174 (1975).
- ⁴⁰K. Taubjerg and P. Sigmund, *Phys. Rev. A* **5**, 1285 (1972); K. Taubjerg, B. Fastrup, and E. Laegsgaard, *Phys. Rev. A* **8**, 1814 (1973).
- ⁴¹H. W. Schnopper, A. R. Sohval, H. D. Betz, J. P. Delvaille, K. Kalata, K. W. Jones, and H. E. Wegner, in *Proceedings of the International Conference on Inner-Shell Ionization Phenomena and Future Applications*, edited by R. W. Fink, S. J. Manson, J. M. Palms, and R. Venugopala Rao (U.S. E.R.D.A., Oak Ridge, 1973), Vol. 3, p. 1348.
- ⁴²L. C. Northcliffe and R. F. Schilling, *Nucl. Data Tables* **7**, 233 (1970).
- ⁴³D. Ward, J. S. Foster, H. R. Andrews, I. V. Mitchell, G. C. Ball, W. G. Davies, and G. J. Costa, Atomic Energy of Canada Limited Reports No. AECL-4914 and 5313, 1975 (unpublished).
- ⁴⁴C. M. Lederer, J. M. Hollander, and I. Perlman, *Table of Isotopes*, 6th ed. (Wiley, New York, 1967), p. 566; B. Fricke and G. Soff, Gesellschaft für Schwerionenforschung, Darmstadt, Germany, Report No. GSI-T1-74, 1974 (unpublished).